Journal of Coordination Chemistry
Publication details, including instructions for authors and subscription information:
http://www.tandfonline.com/loi/gcoo20

Cytotoxicity, apoptosis, interaction with DNA, cellular uptake, and cell cycle arrest of ruthenium(II) polypyridyl complexes containing 4,4′-dimethyl-2,2′-bipyridine as ancillary ligand

Hong-Liang Huang [a], Zheng-Zheng Li [b], Xiu-Zhen Wang [b], Zhen-Hua Liang [b] & Yun-Jun Liu [b]

[a] School of Life Science and Biopharmaceuticals, Guangdong Pharmaceutical University, Guangdong, Guangzhou 510006, P.R. China

[b] School of Pharmacy, Guangdong Pharmaceutical University, Guangdong, Guangzhou 510006, P.R. China

Accepted author version posted online: 19 Jul 2012. Published online: 02 Aug 2012.

To cite this article: Hong-Liang Huang, Zheng-Zheng Li, Xiu-Zhen Wang, Zhen-Hua Liang & Yun-Jun Liu (2012) Cytotoxicity, apoptosis, interaction with DNA, cellular uptake, and cell cycle arrest of ruthenium(II) polypyridyl complexes containing 4,4′-dimethyl-2,2′-bipyridine as ancillary ligand, Journal of Coordination Chemistry, 65:18, 3287-3298, DOI: 10.1080/00958972.2012.713945

To link to this article: http://dx.doi.org/10.1080/00958972.2012.713945

Journal of Coordination Chemistry
Vol. 65, No. 18, 20 September 2012, 3287–3298

Cytotoxicity, apoptosis, interaction with DNA, cellular uptake, and cell cycle arrest of ruthenium(II) polypyridyl complexes containing 4,4′-dimethyl-2,2′-bipyridine as ancillary ligand

HONG-LIANG HUANG†, ZHENG-ZHENG LI‡, XIU-ZHEN WANG‡, ZHEN-HUA LIANG‡ and YUN-JUN LIU*‡

†School of Life Science and Biopharmaceuticals, Guangdong Pharmaceutical University, Guangdong, Guangzhou 510006, P.R. China
‡School of Pharmacy, Guangdong Pharmaceutical University, Guangdong, Guangzhou 510006, P.R. China

(*Received 15 March 2012; in final form 13 June 2012*)

Two new ruthenium(II) polypyridyl complexes, $[Ru(dmb)_2(DNPIP)](ClO_4)_2$ (**1**) (DNPIP = 2-(2,4-dinitrophenyl)imidazo[4,5-*f*][1,10]phenanthroline, dmb = 4,4′-dimethyl-2,2′-bipyridine) and $[Ru(dmb)_2(DAPIP)](ClO_4)_2$ (**2**) (DAPIP = 2-(2,4-diaminophenyl)imidazo[4,5*f*][1,10]phenanthroline), were synthesized and characterized. The DNA-binding behaviors of these complexes have been studied by UV-Vis absorption titration, viscosity measurements, and photocleavage. The DNA-binding constants are 7.39 $(\pm 0.16) \times 10^4$ ($s = 2.68$) and 2.73 $(\pm 0.16) \times 10^4 (\text{mol L}^{-1})^{-1}$ ($s = 0.64$) for **1** and **2**, respectively. Their evaluation as cytotoxic agents on different cancer cell lines was investigated with IC_{50} values of 59.5, 51.3, and 70.3 μmol L^{-1} for **1**, >100, 87.9, and 77.9 μmol L^{-1} for **2** against BEL-7402, HepG-2, and MCF-7 cells, respectively. Complex **1** is more active than **2** against selected cancer cell lines. The apoptosis induced by these complexes was studied. Cellular uptake showed that these complexes could enter into the cytoplasm and accumulate in the nuclei. The cell cycle arrest and antioxidant activity against hydroxyl radicals were also investigated.

Keywords: Ruthenium(II) complex; Cytotoxicity; Apoptosis; Cellular uptake; Cell cycle arrest

1. Introduction

There have been extensive studies on the factors that govern the affinity and specificity of binding of small molecules to DNA, leading to the discovery that molecules bind to DNA by different mechanisms and exert their biological activities [1]. Binding studies of small molecules with deoxyribonucleic acid (DNA) are important in design of new and more efficient drugs targeted to DNA [2, 3]. Small molecular compounds bind to DNA with non-covalent interactions, such as electrostatic binding, groove binding, and intercalative binding. Intercalating and groove binding molecules are important tools in molecular biology and many are clinically useful in the treatment of cancer [4, 5]. Ruthenium polypyridyl complexes bind to DNA by intercalation and some Ru(II)

*Corresponding author. Email: lyjche@163.com

ISSN 0095-8972 print/ISSN 1029-0389 online © 2012 Taylor & Francis
http://dx.doi.org/10.1080/00958972.2012.713945

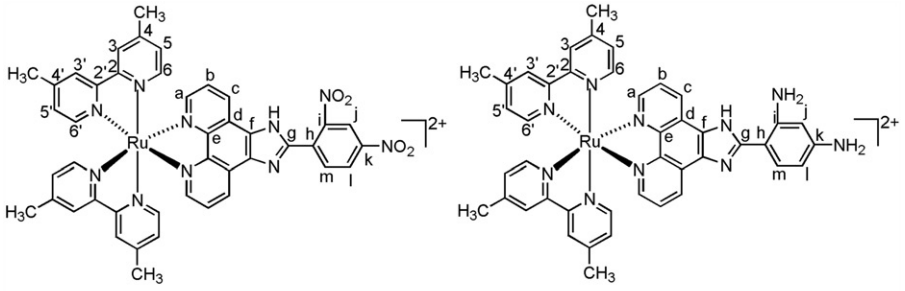

Scheme 1. The structures of **1** and **2**.

complexes act as molecular light switches [6–13]. Studies on biological activity of ruthenium(II) complexes have received attention [14–20]. $[Ru(phen)_2\text{-p-MOPIP}]^{2+}$ can induce mitochondria-mediated and caspase-dependent apoptosis in human cancer cells [17] and $[Ru(bpy)_2(dppn)]^{2+}$ exhibits cytotoxic activity with a low micromolar IC_{50} value [21]. Based on our previous investigation [22, 23], to further understand the relation between structure of ruthenium(II) polypyridyl complexes and biological activities, in this report, we synthesize two new Ru(II) polypyridyl complexes, $[Ru(dmb)_2(DNPIP)](ClO_4)_2$ (**1**) (dmb = 4,4′-dimethyl-2,2′-bipyridine, DNPIP = 2-(2,4-dinitrophenyl)imidazo[4,5-*f*][1,10]phenanthroline) and $[Ru(dmb)_2(DAPIP)](ClO_4)_2$ (**2**) (DAPIP = 2-(2,4-diaminophenyl)imidazo[4,5-*f*][1,10]phenanthroline, scheme 1). Their DNA-binding behaviors were studied by absorption titration, viscosity measurements, and photoactivated cleavage. The biological characteristics of these complexes were also investigated.

2. Materials and methods

2.1. *Materials*

Calf thymus DNA (CT-DNA) was obtained from the Sino-American Biotechnology Company. pBR322 DNA was obtained from Shanghai Sangon Biological Engineering & Services Co., Ltd. Dimethyl sulfoxide (DMSO) and RPMI 1640 were purchased from Sigma. Cell lines of hepatocellular (BEL-7402), hepatocellular (HepG-2), and breast cancer (MCF-7) were purchased from American Type Culture Collection; agarose and ethidium bromide (EB) were obtained from Aldrich. $RuCl_3 \cdot xH_2O$ was purchased from Kunming Institute of Precious Metals. 1,10-Phenanthroline was obtained from Guangzhou Chemical Reagent Factory.

2.2. *Synthesis and characterization of Ru(II) complexes*

2.2.1. Synthesis of $[Ru(dmb)_2(DNPIP)](ClO_4)_2$ (1). A mixture of *cis*-$[Ru(dmb)_2Cl_2] \cdot 2H_2O$ (0.286 g, 0.5 mmol) [24] and DNPIP (0.193 g, 0.5 mmol) [23] in ethylene glycol

($20\,cm^3$) was refluxed under argon for 8 h to give a clear red solution. Upon cooling, a red precipitate was obtained by dropwise addition of saturated aqueous $NaClO_4$ solution. The crude product was purified by column chromatography on neutral alumina with a mixture of CH_3CN–toluene (3 : 1, v/v) as eluent. The red band was collected, solvent removed under reduced pressure, and a red powder was obtained. Yield: 72%. Anal. Calcd for $C_{43}H_{34}N_{10}Cl_2O_{12}Ru$ (%): C, 48.97; H, 3.25; N, 13.28. Found (%): C, 48.65; H, 3.14; N, 13.01. ESI-MS [CH_3CN, m/z]: 855.3 ([M – $2ClO_4$ – H]$^+$), 428.2 ([M – $2ClO_4$]$^{2+}$). ^{1}H NMR (500 MHz, DMSO-d_6): δ 8.80 (d, 1H, H_l, $J = 8.0$ Hz), 8.73 (s, 1H, H_j), 8.67 (d, 1H, H_c, $J = 4.5$ Hz), 8.63 (d, 1H, H_c, $J = 5.0$ Hz), 8.47 (d, 1H, H_m, $J = 6.5$ Hz), 7.80 (d, 2H, H_a, $J = 5.0$ Hz), 7.68 (d, 4H, $H_{6,6'}$, $J = 5.5$ Hz), 7.40 (t, 4H, $H_{3,3'}$, $J = 6.0$ Hz), 7.23 (t, 2H, H_b, $J = 6.5$ Hz), 7.14–7.18 (m, 4H, $H_{5,5'}$), 1.90 (s, 6H, H_{CH3}), 1.75 (s, 6H, H_{CH3}). ^{13}C NMR (DMSO-d_6, ppm): 156.40 C (2), 156.25 C (2′), 150.41 C (6), 150.31 C (6′), 149.35 C (a), 149.18 C (e, k), 147.86 C (i), 147.33 C (4), 144.64 C (g), 129.59 C (c, h), 128.39 C (l), 125.28 C (d, f, m), 124.94 C (3), 119.13 C (b, 5), 118.11 C (j), 20.78 C (CH_3).

2.2.2. Synthesis of $[Ru(dmb)_2(DAPIP)](ClO_4)_2$ (2). A mixture of $[Ru(dmb)_2(DNPIP)](ClO_4)_2$ (**1**) (0.527 g, 0.5 mmol) (dissolved in minimum acetonitrile), Pd/C (0.20 g, 10% Pd), $NH_2NH_2 \cdot H_2O$ ($8\,cm^3$), and ethanol ($20\,cm^3$) were refluxed under argon for 8 h. The hot solution was filtered and evaporated under reduced pressure to reduce the solvent to $6\,cm^3$. Upon cooling, a red precipitate was obtained by dropwise addition of saturated aqueous $NaClO_4$ solution. The crude product was purified by column chromatography on neutral alumina with a mixture of CH_3CN–toluene (3 : 1, v/v) as eluent. The red band was collected. The solvent was removed under reduced pressure and a red powder was obtained. Yield: 70%. Anal. Calcd for $C_{43}H_{38}N_{10}Cl_2O_8Ru$ (%): C, 51.92; H, 3.85; N, 14.08. Found (%): C, 51.68; H, 3.71; N, 13.96. ESI-MS [CH_3CN, m/z]: 795.3 ([M – $2ClO_4$ – H]$^+$), 398.4 ([M – $2ClO_4$]$^{2+}$). ^{1}H NMR (500 MHz, DMSO-d_6): δ 9.06 (d, 2H, H_c, $J = 8.0$ Hz), 8.72 (d, 4H, $H_{6,6'}$, $J = 8.5$ Hz), 8.03 (d, 2H, H_a, $J = 5.0$ Hz), 7.85 (t, 2H, H_b, $J = 5.0$ Hz), 7.66 (d, 4H, $H_{3,3'}$, $J = 5.5$ Hz), 7.34–7.42 (m, 4H, $H_{5,5'}$), 7.15 (d, 1H, H_m, $J = 6.0$ Hz), 6.02–6.06 (m, 1H, H_l), 5.74 (s, 1H, H_j), 5.47 (s, 4H, H_{NH2}), 2.07 (s, 6H, H_{CH3}), 1.75 (s, 6H, H_{CH3}). ^{13}C NMR (DMSO-d_6, ppm): 156.34 C (2), 156.18 C (2′), 155.13 C (6,6′), 151.53 C (a), 150.56 C (4), 150.41 C (4′), 149.69 C (e), 149.55 C (k), 149.39 C (i), 144.75 C (g), 144.19 C (d, f, m), 130.19 C (c), 128.51 C (3), 128.38 C (3′), 125.77 C (5), 125.49 C (5′), 124.99 C (b), 104.00 C (h), 99.58 C (l), 98.76 C (j), 20.78 C (CH_3).

Caution: Perchlorate salts of metal compounds with organic ligands are potentially explosive, and only small amounts of the material should be prepared and handled with great care.

2.3. *Methods*

Doubly distilled water was used to prepare buffers. A solution of CT-DNA in the buffer gave a ratio of UV absorbance at 260 and 280 nm of *ca* 1.8–1.9 : 1, indicating that the DNA was sufficiently free of protein [25]. The DNA concentration per nucleotide was determined by absorption spectroscopy using the molar absorption coefficient ($6600\,(mol\,L^{-1})^{-1}\,cm^{-1}$) at 260 nm [26].

Microanalysis (C, H, and N) was carried out with a Perkin-Elmer 240Q elemental analyzer. Electrospray mass spectra (ESI-MS) were recorded on an LCQ system (Finnigan MAT, USA) using methanol as the mobile phase. The spray voltage, tube lens offset, capillary voltage, and capillary temperature were set at 4.50 kV, 30.00 V, 23.00 V and 200°C, respectively, and the quoted m/z values are for the major peaks in the isotope distribution. ^{1}H NMR spectra were recorded on a Varian-500 spectrometer. All chemical shifts are given relative to tetramethylsilane (TMS). UV-Vis spectra were recorded on a Shimadzu UV-3101PC spectrophotometer at room temperature.

2.4. *DNA-binding studies*

DNA-binding was performed at room temperature. Buffer (5 mmol L^{-1} tris(hydroxymethyl)aminomethane (Tris) hydrochloride, 50 mmol L^{-1} NaCl, pH 7.0) was used for absorption titration and viscosity measurements. Viscosity measurements were carried out using an Ubbelodhe viscometer maintained at 25.0 (±0.1)°C in a thermostatic bath. DNA samples approximately 200 base pairs in average length were prepared by sonication to minimize complexities arising from DNA flexibility [27]. Flow time was measured with a digital stopwatch, each sample was measured three times, and an average flow time was calculated. Relative viscosities for DNA in the presence and absence of complexes were calculated from the relation $\eta = (t - t^0)/t^0$, where t is the observed flow time of the DNA-containing solution and t^0 is the flow time of buffer alone [28, 29]. Data are presented as $(\eta/\eta_0)^{1/3}$ *versus* binding ratio ($r = 0.04$, 0.08, 0.12, and 0.16) [30], where η is the viscosity of DNA in the presence of complexes and η_0 is the viscosity of DNA alone.

The absorption titrations of the complex in buffer were performed using a fixed concentration (20 μmol L^{-1}) for complex to which increments of DNA stock solution were added. Ru-DNA solutions were allowed to incubate for 5 min before the absorption spectra were recorded. The intrinsic binding constants K, based on the absorption titration, were measured by monitoring changes in absorption at the metal-to-ligand charge transfer (MLCT) band with increasing concentration of DNA using the following equation [31],

$$(\varepsilon_a - \varepsilon_f)/(\varepsilon_b - \varepsilon_f) = (b - (b^2 - 2K^2C_t[\mathrm{DNA}]/s))^{1/2}/2KC_t, \quad (1a)$$

$$(b = 1 + KC_t + K[\mathrm{DNA}]/2s), \quad (1b)$$

where [DNA] is the concentration of CT-DNA in base pairs, the apparent absorption coefficients ε_a, ε_f, and ε_b correspond to $A_{obsd}/[\mathrm{Ru}]$, the absorbance for the free ruthenium complex, and the absorbance for the ruthenium complex in fully bound form, respectively. K is the equilibrium binding constant, C_t is the total concentration of metal complex, and s is the binding site size.

2.5. *Scavenger measurements of hydroxyl radical (•OH)*

The hydroxyl radical (•OH) in aqueous media was generated by the Fenton system [32]. The solution of the tested complexes was prepared with DMF (N,N-dimethylformamide). An assay mixture of 5 mL contained the following reagents: safranin

($28.5\,\mu mol\,L^{-1}$), EDTA-Fe(II) ($100\,\mu mol\,L^{-1}$), H_2O_2 ($44.0\,\mu mol\,L^{-1}$), the tested compounds ($0.5–3.5\,\mu mol\,L^{-1}$), and a phosphate buffer ($67\,mmol\,L^{-1}$, pH = 7.4). The assay mixtures were incubated at 37°C for 30 min in a water bath and the absorbance was measured at 520 nm. All tests were run in triplicate and expressed as the mean. A_i was the absorbance in the presence of the tested compound; A_0 was the absorbance in the absence of tested compounds; and A_c was the absorbance in the absence of tested compound, EDTA-Fe(II), H_2O_2. The suppression ratio (η_a) was calculated on the basis of $(A_i - A_0)/(A_c - A_0) \times 100\%$.

2.6. *Cytotoxicity assay* in vitro

Standard 3-(4,5-dimethylthiazole)-2,5-diphenyltetrazolium bromide (MTT) assay procedures were used [33]. Cells were placed in 96-well microassay culture plates (8×10^3 cells per well) and grown overnight at 37°C in a 5% CO_2 incubator. The complexes tested were dissolved in DMSO and diluted with RPMI 1640 and then added to the wells to achieve final concentrations ranging from 10^{-6} to $10^{-4}\,mol\,L^{-1}$. Control wells with cells were prepared by addition of culture medium (100 μL). Wells containing culture medium without cells were used as blanks and cisplatin was used as positive control. The plates were incubated at 37°C in a 5% CO_2 incubator for 72 h. Upon completion of the incubation, stock MTT dye solution (20 μL, $5\,mg\,mL^{-1}$) was added to each well. After 4 h incubation, buffer (100 μL) containing N,N-dimethylformamide (50%) and sodium dodecyl sulfate (20%) was added to solubilize the MTT formazan. The optical density of each well was then measured on a microplate spectrophotometer at 490 nm. The IC_{50} values were determined by plotting the percentage viability *versus* concentration on a logarithmic graph and reading off the concentration at which 50% of cells remain viable relative to the control. Each experiment was repeated at least three times to get the mean values. Three different tumor cell lines were the subject of this study: BEL-7402, HepG-2, and MCF-7.

2.7. *Apoptosis assessment by acridine orange/EB staining*

Apoptosis studies were performed with a staining method utilizing acridine orange (AO) and EB [34]. AO can pass through cell membrane, but EB cannot. Under fluorescence microscope, live cells appear green. Necrotic cells stain red but have a nuclear morphology resembling that of viable cells. Apoptotic cells appear green, and morphological changes such as cell blebbing and formation of apoptotic bodies will be observed. A monolayer of BEL-7402 cells was incubated in the absence and presence of **2** at $50\,\mu mol\,L^{-1}$ at 37°C and 5% CO_2 for 48 h. Then each cell culture was stained with AO/EB solution ($100\,\mu g\,mL^{-1}$ AO, $100\,\mu g\,mL^{-1}$ EB). Samples were observed under a fluorescence microscope.

2.8. *Cellular uptake study*

Cells were placed in 24-well microassay culture plates (4×10^4 cells per well) and grown overnight at 37°C in a 5% CO_2 incubator. Complex **2** was then added to the wells. The plates were incubated at 37°C in a 5% CO_2 incubator for 24 h. Then the wells were

washed three times with phosphate buffered saline (PBS), after removing the culture medium, the cells were visualized by fluorescence microscopy.

2.9. *Cell cycle arrest*

HepG-2 cells were seeded into six-well plates (Costar, Corning Corp., New York) at a density of 2×10^5 cells per well and incubated for 24 h. The cells were cultured in RPMI 1640 supplemented with fetal bovine serum (10% FBS) and incubated at 37°C and 5% CO_2. The medium was removed and replaced with medium (final DMSO concentration, 1% v/v) containing **1** (50 μmol L^{-1}). After incubation for 24 h, the cell layer was trypsinized, washed with cold PBS, and fixed with 70% ethanol. 20 mL of RNAse (0.2 mg mL^{-1}) and 20 mL of propidium iodide (PI, 0.02 mg mL^{-1}) were added to the cell suspensions and incubated at 37°C for 30 min. Then the samples were analyzed by an FACS Calibur flow cytometer (Becton Dickinson & Co., Franklin Lakes, NJ). The number of cells analyzed was 10,000 [35].

3. Results and discussion

3.1. *Synthesis and characterization*

DNPIP was synthesized by refluxing a mixture of 1,10-phenanthroline-5,6-dione and 2,4-dinitrobenzaldehyde following a similar method described by Steck and Day [36]. $[Ru(dmb)_2(DNPIP)](ClO_4)_2$ (**1**) was prepared by direct reaction of DNPIP with $[Ru(dmb)_2Cl_2] \cdot 2H_2O$ in ethylene glycol in relatively high yield. $[Ru(dmb)_2(DAPIP)](ClO_4)_2$ (**2**), was synthesized by reducing **1** in the presence of Pd/C and $NH_2NH_2 \cdot H_2O$ in ethanol. The desired Ru(II) complexes were isolated as the perchlorates and purified by column chromatography. In ^1H NMR spectra, the chemical shift of H_j in DNPIP is 9.06 ppm [23], a shift of 0.33 in **1** and 3.32 ppm in **2** for H_j was observed (figure S1). In the ES-MS of **1** and **2**, all of the expected signals $[M - 2ClO_4 - H]^+$ and $[M - 2ClO_4]^{2+}$ were observed (figure S2). The measured molecular masses were consistent with expected values.

Electronic absorbance spectra of the complexes in DMSO were characterized by an intense ligand-centered transition in the UV and an MLCT transition in the visible region. In the UV region, intense, fairly sharp bands at 288 nm for **1** and 289 nm for **2** are assigned as intraligand π–π^* transitions. Low-energy absorptions at 480 and 456 nm for **1** and **2**, respectively, are attributed to the MLCT transition by comparison with spectra of other ruthenium(II) complexes [37–39] (figure S3).

3.2. *Electronic absorption spectra titration*

Generally, the ligand-centered $\pi \rightarrow \pi^*$ and MLCT absorptions shift to longer wavelengths (bathochromism) and decrease in intensity (hypochromism) with increasing concentration of CT-DNA [40]. Figure 1 shows the absorption spectra of **1** and **2** in the presence of increasing concentrations of DNA. With increasing concentrations of CT-DNA, the MLCT bands of **1** at 467 and **2** at 466 nm exhibit hypochromism of 41.2

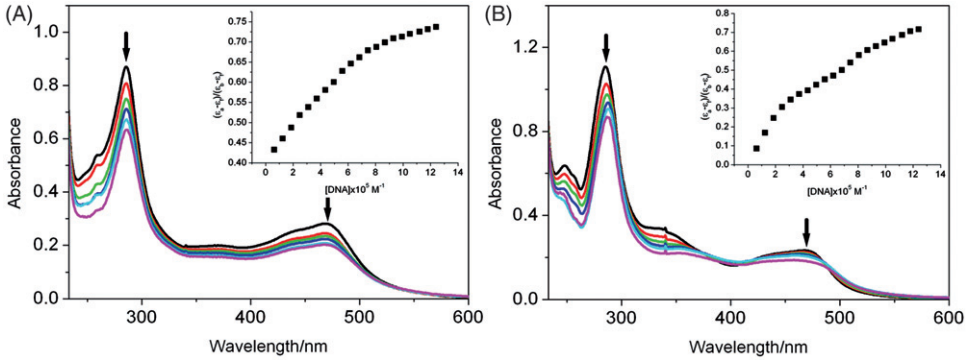

Figure 1. Absorption spectra of **1** (A) and **2** (B) in Tris-HCl buffer upon addition of CT-DNA. [Ru] = 20 μmol L^{-1}. The arrow shows the absorbance change upon increase of DNA concentration. Plots of $(\varepsilon_a - \varepsilon_f)/(\varepsilon_b - \varepsilon_f)$ *vs.* [DNA] for titration of DNA with Ru(II) complexes.

and 21.79%, and bathochromism of 3 and 2 nm, respectively. These spectral characteristics suggest that the complexes interact with DNA through a mode that involves a stacking interaction between the aromatic chromophore and the base pairs of DNA. In order to elucidate the DNA-binding strength of **1** and **2** with DNA, the DNA-binding constants K_b were determined by monitoring the changes in absorbance of the MLCT band with increasing concentrations of CT-DNA. The values of K_b were $7.4\ (\pm 0.2) \times 10^4$ ($s = 2.68$) and $2.7\ (\pm 0.2) \times 10^4 (\text{mol L}^{-1})^{-1}$ ($s = 0.64$) for **1** and **2**, respectively. The value of K_b for **1** is larger than that of **2**, caused by the electron-withdrawing substituent ($-NO_2$ in DNPIP) on the intercalative ligand improving the DNA-binding affinity, and the electron-pushing substituent ($-NH_2$ in DAPIP) decreasing the DNA affinity.

3.3. *Viscosity measurements*

Viscosity measurements of DNA are regarded as the least ambiguous and the most critical test of a DNA-binding model in solution and provide strong arguments for intercalative DNA-binding mode [28, 29]. Intercalators unwind the double helix when they insert between DNA base pairs, producing DNA that is somewhat elongated relative to canonical B-form DNA. Lengthening of the helical axis gives measurable increases in viscosities [41] that are not observed for groove binding or electrostatic association. The effects of **1** and **2** on the relative viscosity of rod-like DNA are shown in figure 2. With increasing concentrations of **1** and **2**, the relative viscosity of the DNA solution increased steadily. The increasing relative viscosity of DNA for **1** is larger than that for **2**, attributed to the different DNA-binding affinity of the two complexes. Considering the DNA-binding affinities and the changes in viscosity, **1** and **2** interact with CT-DNA by groove binding.

3.4. *Antioxidant activity against hydroxyl radical*

Increasing spectrum of diseases as well as aging has been a subject of antioxidant supplementation. Among all reactive oxygen species the hydroxyl radical (•OH) is by

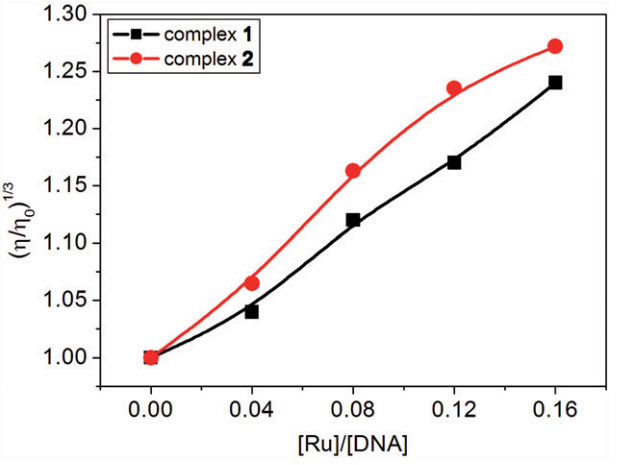

Figure 2. Effect of increasing amounts of **1** (•) and **2** (■) on the relative viscosity of CT-DNA at 25 (±0.1)°C. [DNA] = 0.25 mmol L^{-1}.

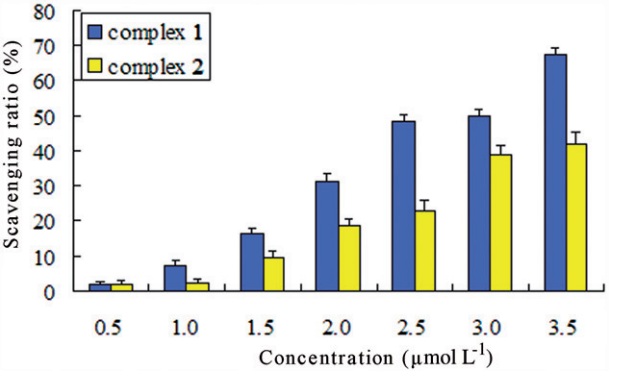

Figure 3. Scavenging effect of **1** and **2** on hydroxyl radicals. Experiments were performed in triplicate.

Table 1. The scavenging ratios (%) of ligand and complexes against •OH.

	Average inhibition (%) for •OH						
Compound	0.5	1.0	1.5	2.0	2.5	3.0	3.5 (μmol L^{-1})
1	1.6 ± 0.6	7.3 ± 1.4	16.2 ± 2.1	31.3 ± 2.2	48.4 ± 3.1	50.1 ± 3.2	67.2 ± 3.3
2	1.8 ± 0.7	2.1 ± 1.1	9.6 ± 1.7	18.5 ± 2.0	22.9 ± 3.2	38.9 ± 3.4	42.2 ± 3.6

far the most potent and dangerous oxygen metabolite; elimination of this radical is one of the main aims of antioxidant administration [42]. The antioxidant activities of **1** and **2** are shown in figure 3 and table 1. The suppression ratio against •OH varied from 1.11 to 67.19 for **1** and 1.82 to 42.19 for **2**. The inhibitory effect of these complexes on •OH was concentration-dependent and the suppression ratio increased with increase in

Table 2. The IC_{50} values of **1** and **2** on the selected cell lines.

	IC_{50} ($\mu mol\,L^{-1}$)		
Compound	BEL-7402	HepG-2	MCF-7
1	59.5 ± 3.5	51.3 ± 5.0	70.3 ± 3.4
2	>100	87.9 ± 3.3	77.9 ± 2.4
Cisplatin	19.8 ± 2.6	25.5 ± 3.2	9.7 ± 2.6

sample concentrations from 0.5 to 3.5 $\mu mol\,L^{-1}$. Comparing the suppression ratio of **1** and **2**, the antioxidant activity of **1** is higher than that of **2** under the same conditions.

3.5. *Cytotoxicity assay*

The cytotoxicities of **1** and **2** were evaluated on BEL-7402 (hepatocellular), HepG-2 (hepatocellular), and MCF-7 (breast cancer) by cell survival after 72 h of exposure using the MTT assay. Cisplatin was used as positive control. The concentrations varied from 6.25 to 400 $\mu mol\,L^{-1}$ and IC_{50} values calculated after 72 h of incubation with **1** and **2** are listed in table 2. The cell viability was concentration-dependent, and increasing the concentrations of **1** and **2** caused a decrease in cell viability. Comparing the IC_{50} values (table 2), **1** shows higher activity than **2** against selected tumor cell lines, but their cytotoxic activities are far lower than that of cisplatin.

3.6. *Apoptosis activity studies*

In order to gain some insight into cell death type induced by **2**, the apoptosis assays were performed on BEL-7402 cells with AO and EB staining. Cells sensing an inflicted aggression by a chemical compound undergo two major forms of death, necrosis or apoptosis, and each with very distinct characteristics. The control and treatment of BEL-7402 cells with **2** are shown in figure 4. In the absence of **2**, the living cells were stained bright green in spots (figure 4A). However, after treatment with **2**, the green apoptotic cells containing apoptotic bodies, as well as red necrotic cells, were also observed (figure 4B). The results show **2** can effectively induce apoptosis.

3.7. *Cellular uptake studies*

In the functional study, cellular uptake of **2** (50 $\mu mol\,L^{-1}$) by BEL-7402 cells was studied using fluorescence microscopy. In control experiments, BEL-7402 cells do not show luminescence (data not presented). After treatment of BEL-7402 cells with **2**, bright red fluorescence spots in the images were observed (figure 5). The result showed that **2** can be uptaken by BEL-7402 cells, enter into the cytoplasm, and accumulate in the nuclei.

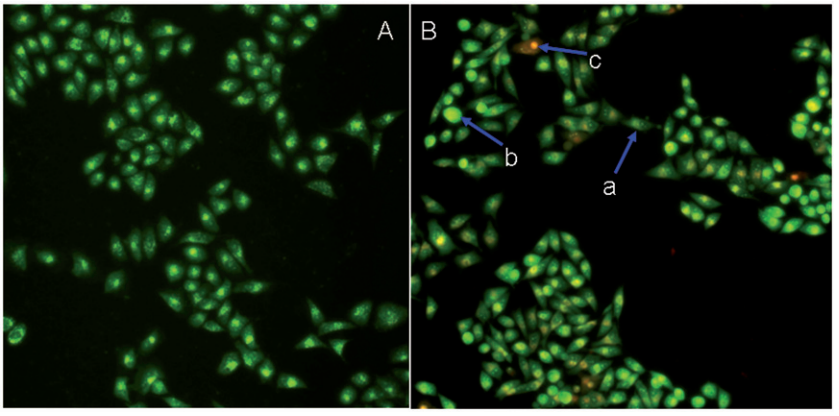

Figure 4. BEL-7402 cells were stained by AO/EB and observed under fluorescence microscopy. BEL-7402 cells without treatment (A) and in the presence of **2** (B) incubated at 37°C and 5% CO_2 for 48 h. Cells in a, b, and c are living, apoptotic, and necrotic cells, respectively.

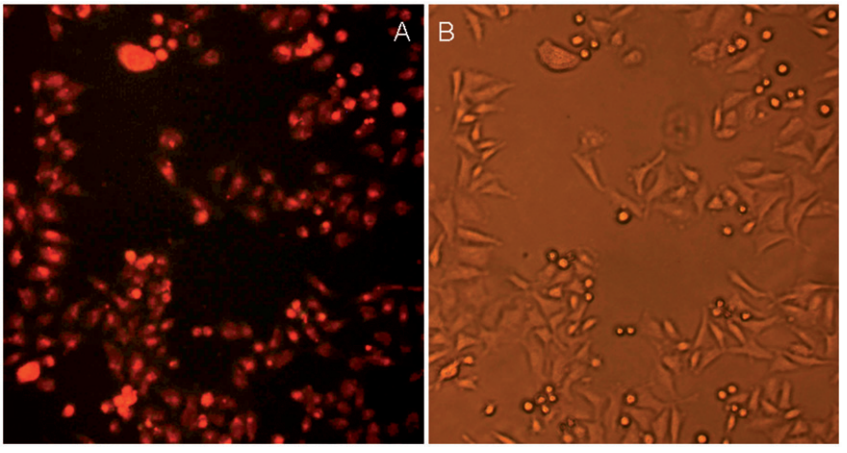

Figure 5. BEL-7402 cells incubated with **2** (50 μmol L^{-1}) for 24 h imaged by fluorescence microscopy. Note that the cytoplasm is extensively stained with the Ru(II) complexes.

3.8. *Flow cytometric analysis*

A better understanding of the mechanism of drug-induced cytotoxicity is important in the design of more effective chemotherapeutic agents. Inhibition of cancer cell proliferation by cytotoxic drugs could result from induction of apoptosis or of cell cycle arrest [43]. The effect of **1** on cell cycle of HepG-2 cells was investigated by flow cytometry in PI (propidium iodide) stained cells after Ru(II) complex treatment for 24 h. Representative DNA distribution histograms of HepG-2 cells in the absence and presence of **1** are shown in figure 6. Treatment of HepG-2 cells with **1** caused an increase (8.55%) in the percentage of cells at the S-phase, accompanied by corresponding reduction (10.08%) in the G0/G1-phase. The results indicate that **1** can inhibit the cell division in the S-phase on HepG-2 cells.

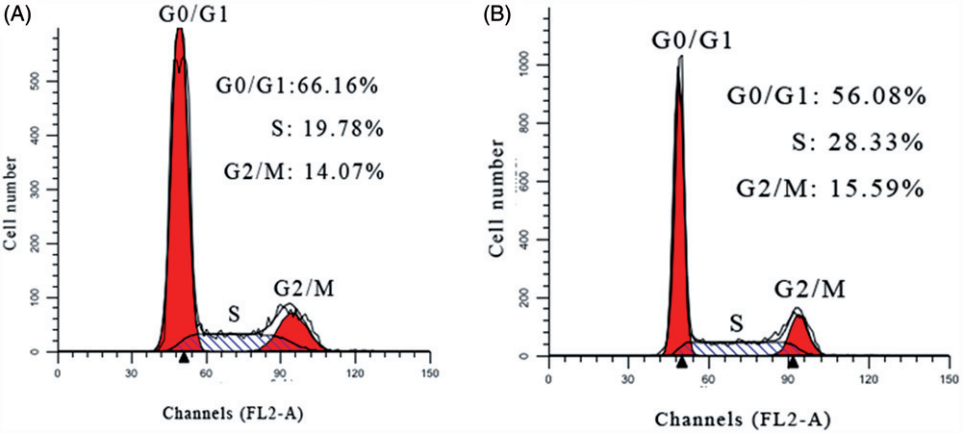

Figure 6. Cell cycle status of HepG-2 cells after treatment with **1** (50 μmol L^{-1}) for 24 h: (A) control; and (B) (**1** + HepG-2).

4. Conclusion

Complexes **1** and **2** bind to CT-DNA by DNA groove binding. Complex **1** shows higher cytotoxicity than **2** on selected tumor cell lines, consistent with the DNA-binding affinities of the two complexes. Complex **2** can effectively induce apoptosis after treatment of BEL-7402 cells. The results obtained from cellular uptake showed that **2** can enter into the cytoplasm and accumulate in the nuclei. Flow cytometric analysis suggested that **1** can inhibit the S-phase transition on HepG-2 cells.

Acknowledgments

This work was supported by the National Nature Science Foundation of China (Nos 31070858, 30800227) and Guangdong Pharmaceutical University.

References

[1] R. Sinha, M.M. Islam, K. Bhadra, G.S. Kumar, A. Banerjee, M. Maiti. *Bioorg. Med. Chem.*, **14**, 800 (2006).
[2] M.P. Singh, T. Joseph, S. Kumar, Y. Bathini, J.W. Lown. *Chem. Res. Toxicol.*, **5**, 597 (1992).
[3] K.E. Rao, J.W. Lown. *Chem. Res. Toxicol.*, **4**, 661 (1991).
[4] M.J. Waring. *Annu. Rev. Biochem.*, **50**, 159 (1981).
[5] P.B. Dervan. *Bioorg. Med. Chem.*, **9**, 2215 (2001).
[6] L.F. Tan, J.L. Shen, X.H. Liu, X.L. Liang. *DNA Cell Biol.*, **28**, 461 (2009).
[7] D. Chatterjee, A. Sengupta, R. van Eldik. *J. Coord. Chem.*, **64**, 30 (2011).
[8] H.L. Huang, Y.J. Liu, C.H. Zeng, L.X. He, F.H. Wu. *DNA Cell Biol.*, **29**, 261 (2010).
[9] X.L. Hong, Z.H. Liang, M.H. Zeng. *J. Coord. Chem.*, **64**, 3792 (2011).
[10] X.W. Liu, Y.M. Shen, J.L. Lu, Y.D. Chen, D.S. Zhang. *Spectrochim. Acta, Part A*, **77**, 522 (2010).
[11] A.E. Friedman, J.C. Chambron, J.P. Sauvage, N.J. Turro, J.K. Barton. *J. Am. Chem. Soc.*, **112**, 4960 (1980).

[12] F. Gao, H. Chao, F. Zhou, Y.X. Yuan, B. Peng, L.N. Ji. *J. Inorg. Biochem.*, **100**, 1487 (2006).
[13] X.W. Liu, L. Lin, J.L. Lu, Y.D. Chen, D.S. Zhang. *J. Coord. Chem.*, **64**, 4344 (2011).
[14] Y.J. Liu, C.H. Zeng, H.L. Huang, L.X. He, F.H. Wu. *Eur. J. Med. Chem.*, **45**, 564 (2010).
[15] T.F. Chen, Y.N. Liu, W.J. Zheng, J. Liu, Y.S. Wong. *Inorg. Chem.*, **49**, 6366 (2010).
[16] Y.J. Liu, C.H. Zeng, J.H. Yao, F.H. Wu, L.X. He, H.L. Huang. *Chem. Biodivers.*, **7**, 1770 (2010).
[17] C.A. Puckett, J.K. Barton. *Bioorg. Med. Chem.*, **18**, 3564 (2010).
[18] L. Xu, N.J. Zhong, Y.Y. Xie, H.L. Huang, Z.H. Liang, Z.Z. Li, Y.J. Liu. *J. Coord. Chem.*, **65**, 55 (2012).
[19] C.A. Puckett, J.K. Barton. *Biochemistry*, **47**, 11711 (2008).
[20] Q.F. Guo, S.H. Liu, Q.H. Liu, H.H. Xu, J.H. Zhao, H.F. Wu, X.Y. Li, J.W. Wang. *J. Coord. Chem.*, **65**, 1781 (2012).
[21] U. Schatzschneider, J. Niesel, I. Ott, R. Gust, H. Alborzinia, S. Wölfl. *ChemMedChem*, **3**, 1104 (2008).
[22] Y.J. Liu, Z.Z. Li, Z.H. Liang, J.H. Yao, H.L. Huang. *DNA Cell Biol.*, **30**, 839 (2011).
[23] H.L. Huang, Z.Z. Li, Z.H. Liang, J.H. Yao, Y.J. Liu. *Eur. J. Med. Chem.*, **46**, 3282 (2011).
[24] B.P. Sullivan, D.J. Salmon, T.J. Meyer. *Inorg. Chem.*, **17**, 3334 (1978).
[25] J. Marmur. *J. Mol. Biol.*, **3**, 208 (1961).
[26] M.E. Reichmann, S.A. Rice, C.A. Thomas, P. Doty. *J. Am. Chem. Soc.*, **7**, 3047 (1954).
[27] J.B. Chaires, N. Dattagupta, D.M. Crothers. *Biochemistry*, **21**, 3933 (1982).
[28] S. Satyanarayana, J.C. Dabrowiak, J.B. Chaires. *Biochemistry*, **32**, 2573 (1993).
[29] S. Satyanarayana, J.C. Dabrowiak, J.B. Chaires. *Biochemistry*, **31**, 9319 (1992).
[30] G. Cohen, H. Eisenberg. *Biopolymers*, **8**, 45 (1969).
[31] M.T. Carter, M. Rodriguez, A. Bard. *J. Am. Chem. Soc.*, **111**, 8901 (1989).
[32] C.C. Cheng, S.E. Rokita, C.J. Burrows. *Angew. Chem. Int. Ed. Engl.*, **32**, 277 (1993).
[33] T. Mosmann. *J. Immunol. Methods*, **65**, 55 (1983).
[34] D.L. Spector, R.D. Goldman, L.A. Leinwand. *Cells: A Laboratory Manual*, Vol. 1, Cold Spring Harbor Laboratory Press, New York (1998).
[35] K.K. Lo, T.K. Lee, J.S. Lau, W.L. Poon, S.H. Cheng. *Inorg. Chem.*, **47**, 200 (2008).
[36] E.A. Steck, A.R. Day. *J. Am. Chem. Soc.*, **65**, 452 (1943).
[37] Y.J. Liu, J.F. He, J.H. Yao, W.J. Mei, F.H. Wu, L.X. He. *J. Coord. Chem.*, **32**, 665 (2009).
[38] H.J. Yu, S.M. Huang, L.Y. Li, H.N. Ji, H. Chao, Z.W. Mao, J.Z. Liu, L.N. Ji. *J. Inorg. Biochem.*, **103**, 881 (2009).
[39] H.L. Huang, Z.Z. Li, Z.H. Liang, Y.J. Liu. *Eur. J. Inorg. Chem.*, 5538 (2011).
[40] S. Monro, J. Scott, A. Chouai, R. Lincoln, R. Zong, R.P. Thummel, S.A. McFarland. *Inorg. Chem.*, **49**, 2889 (2010).
[41] H.Q. Liu, B.C. Tzeng, Y.S. You, S.M. Peng, H.L. Chen, M.S. Yang, C.M. Che. *Inorg. Chem.*, **41**, 3161 (2002).
[42] N. Udilova, A.V. Kozlov, W. Bieberschulte, K. Frei, K. Ehrenberger, H. Nohl. *Biochem. Pharmacol.*, **65**, 59 (2003).
[43] T. Chen, Y.S. Wong. *J. Agric. Food Chem.*, **56**, 10574 (2008).